Preprint 35th EUPVSEC 2018

EVIDENCE OF REAR SURFACE RELATED DEGRADATION IN Cz-Si PERC-TYPE SOLAR CELLS

A. Herguth, C. Derricks, D. Sperber
University of Konstanz, Department of Physics, Universitätsstr. 10, 78457 Konstanz, Germany

ABSTRACT: A degradation phenomenon of unknown origin during an accelerated aging test comprising illuminated annealing is observed for boron-doped PERC-type solar cells with SiO_x/SiN_x:H rear surface passivation. By collating different measurement techniques and simulations, the rear surface passivation is identified as component responsible for the observed degradation. The observed degradation on solar cell level shows similarities to the degradation of similar passivation layers in lifetime studies.
Keywords: silicon solar cell, PERC, rear surface passivation, degradation, surface related degradation

1 INTRODUCTION

The efficiency potential of bifacially contacted silicon solar cells with front-side emitter strongly correlates with rear side passivation quality, quantified by the rear side surface recombination velocity S_{rear}, and material quality, quantified by excess carrier lifetime τ_{bulk}, as discussed with regard to open circuit voltage V_{oc} in the context of Fig. 3.

For quite a long time, a full area alloyed rear side contact was standard in p-type solar cell mass production. The alloying process with a typically screen-printed aluminum layer results in a highly Al doped region underneath the actual contact thus forming a high-low junction with the typical lowly p-type doped substrate. The concentration gradient of majority charge carriers and the resulting diffusion leads to the formation of an electric field which repels electrons, being the minority charge carrier species, from the back side (back surface field). Hence, the high-low junction acts as field-effect passivation for the otherwise strongly recombination active silicon-metal contact. Unfortunately, excess charge carrier lifetime in this highly-doped region is quite low and thus effective S_{rear} values for this technology typically exceed 200 cm/s with hardly any room for improvement.

Hence, further improvement requires a disruptive change in cell architecture. The passivated emitter and rear cell (PERC) architecture replaces the full area alloyed high-low junction as both passivation and contact component by a separated large area dielectric passivation (>90% of area) interrupted only by locally Al alloyed contacts (<10% of area). Even though high-low junction passivation quality of the locally Al alloyed contacts might be inferior to the full area alloyed scenario, the strongly reduced area fraction reduces the effective S_{rear} to values well below 100 cm/s thanks to the superior performing dielectric passivation with S being typically < 10 cm/s. Passivation by dielectric layers works by a combination of both chemical passivation of electronic states in the band gap at the silicon-dielectric interface and field effect passivation due to fixed charges in the layers preventing charge carriers in the substrate from recombination at the residual defect states at the silicon-dielectric interface.

However, passivation quality of different dielectric layers or stacks involving hydrogen-rich silicon-nitride layers were found in various lifetime studies to be instable during illuminated annealing even at low temperatures [1-3], hence raising the question if dielectric passivation in PERC-type solar cells might be affected as well, leading inevitably to a degradation of electrical entities like open circuit voltage V_{oc}, short circuit-current density j_{sc} and in consequence also of the conversion efficiency.

Within this contribution, long-term stability of PERC-type solar cells with a passivation layer stack consisting of silicon-oxide (SiO_x) capped by hydrogen-rich silicon-nitride (SiN_x:H) with regard to illuminated annealing is investigated.

2 SAMPLES AND SETUP

A commercially available PERC-type solar cell made of boron-doped Cz-silicon (1.3 Ωcm, 145 µm thickness) with SiO_x/SiN_x:H passivation layer stack at the rear side is used. Although the actual peak temperature of the solar cell during contact firing of the screen-printed contacts is unknown, the formation of Ag front and Al rear contacts implies an actual peak firing temperature above 700°C.

The sample is exposed to an accelerated aging test comprising illuminated annealing at 150°C and 1 sun halogen lamp illumination (j_{sc} equivalent [4]) on a hotplate. Treatment is interrupted every once in a while to measure a current-voltage characteristic yielding V_{oc} and j_{sc} under standard test conditions (STC, 25°C, AM 1.5g spectrum) and monitor the short- and long-term stability.

At the end of the measurement series the solar cell was etched back to the bulk substrate, cleaned in Piranha solution (H_2O_2, H_2SO_4, 80°C), HF-dipped and wet chemically re-passivated using a 0.8 molar iodine-ethanol solution. Effective lifetime was measured by a photoconductance decay (PCD) technique using a WCT120 lifetime tester from Sinton Instruments.

An additional lifetime sample was prepared with both-sided SiO_x/SiN_x:H passivation layer and fired at a peak temperature typical for screen-printed PERC-type solar cells. Again, this sample was exposed to the same illuminated annealing conditions and the effective lifetime was monitored by PCD.

3 RESULTS

Figure 1 shows the evolution of V_{oc} as well as j_{sc} for the solar cell during the accelerated aging test. V_{oc} as well as j_{sc} show a weak drop around 0.1 h which is attributed to a decrease in bulk lifetime due to boron-oxygen related degradation (BO-LID) as was expectable for the used oxygen-rich Cz-material [5,6]. Subsequently V_{oc} and j_{sc} recover from BO-LID as the conditions of the accelerated aging test (excess charge carrier injection at elevated temperature) promote a regeneration (BO-LIR) [6,7]. However, V_{oc} and j_{sc} drop for a second time in long-term leading to losses in V_{oc} of ~20 mV and j_{sc} of ~0.4 mA/cm².

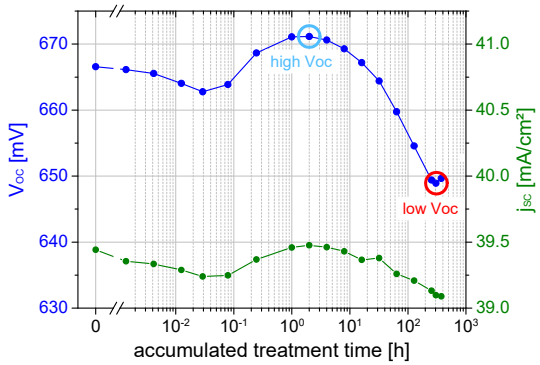

Figure 1: Open-circuit voltage V_{oc} and short-circuit current density j_{sc} measured under standard test conditions during the accelerated aging test.

Only based on these observations, it is hard to decide which cell component is responsible for this second degradation. Therefore, a detailed analysis was carried out which is described in detail elsewhere [8], whereas in this contribution only the major findings are presented. In the following, measurement data taken before the second degradation (~2 h) featuring still a high V_{oc} (and j_{sc}) and after second degradation (~300 h) featuring then a low V_{oc} (and j_{sc}) are compared.

In principle four cell components might be suspected to cause this degradation: defect formation in the emitter or deterioration of front side passivation, defect formation or in-diffusion of contaminants into the space charge region (SCR), defect formation in the bulk and deterioration of rear surface passivation. As the detailed analysis has shown [8], neither changes in the emitter or space charge region are likely and this part of the analysis is therefore not presented here.

Quantum efficiency measurements in the high V_{oc} and low V_{oc} state (shown in Fig. 2) prove that the observed degradation affects the long wavelength regime where light is absorbed deep in the bulk close to the rear surface as seen from the comparison of effective absorption length and cell thickness. Unfortunately, quantum efficiency analysis can virtually not distinguish between a degradation of bulk lifetime, meaning minority carriers more likely get lost in the bulk on their way to the emitter, and a deterioration of rear surface passivation quality, meaning these minority carriers get lost at the rear side [8].

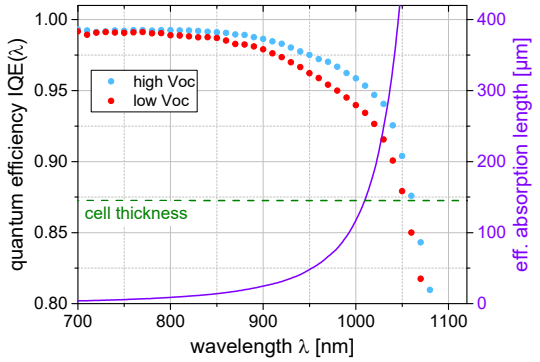

Figure 2: Wavelength-dependent internal quantum efficiency in the high V_{oc} and low V_{oc} state and effective absorption length in the long-wavelength regime.

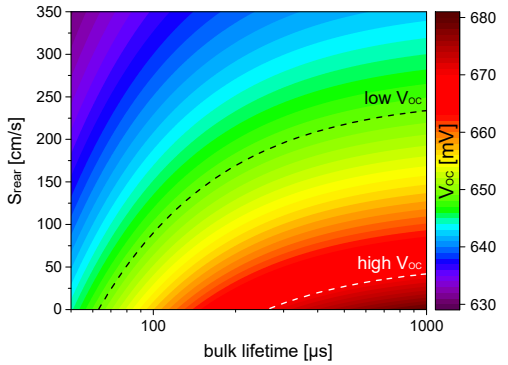

Figure 3: Calculated contour plot of open-circuit voltage V_{oc} in dependence of bulk lifetime (τ_{bulk}) and rear surface recombination velocity (S_{rear}) for the bifacially contacted, front emitter solar cell under investigation. Highlighted contour lines represent combinations of τ_{bulk} and S_{rear} that yield 'low V_{oc}' and 'high V_{oc}' of the investigated sample.

Figure 3 shows a contour plot of V_{oc} versus bulk lifetime τ_{bulk} and rear surface recombination velocity S_{rear} adapted to the specific cell properties. It should be highlighted that both $\tau_{bulk}(\Delta n)$ and $S_{rear}(\Delta n)$ probably depend on injection level Δn and that the specific τ_{bulk} and S_{rear} in Fig. 3 relate to whatever Δn is present at V_{oc}. The highlighted constant V_{oc} contour lines for high V_{oc} and low V_{oc} define possible combinations of τ_{bulk} and S_{rear}, but V_{oc} analysis is not capable of sorting out whether τ_{bulk} has decreased or S_{rear} has increased.

In order to resolve this issue, the solar cell was etched back to the substrate and wet-chemically re-passivated as described above. Figure 4 shows the obtained injection-dependent effective lifetime data. It should be noted that this effective lifetime data is influenced by both bulk lifetime and surface recombination limited lifetime and thus represents only a lower limit for actual bulk lifetime. From the measured low V_{oc} of ~650 mV in the degraded state it can be concluded that injection level is approx. $8.3 \cdot 10^{14}$ cm^{-3} thus the lifetime of ~600 µs at this injection is relevant for comparison with Fig. 3.

The high lifetime after re-passivation restricts possible changes between the high V_{oc} and low V_{oc} contour line in Fig. 3 almost completely to vertical changes suggesting a deterioration of surface passivation quality and excluding a degradation of bulk lifetime.

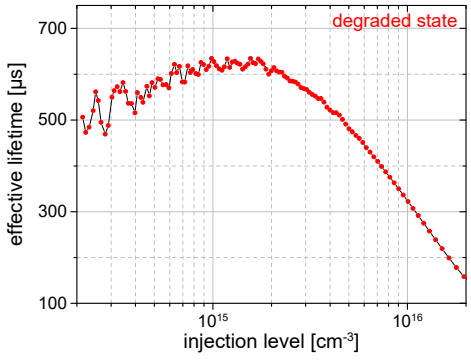

Figure 4: Injection-dependent lifetime data measured via PCD of the stripped and re-passivated solar cell. Low V_{oc} implies an injection level of $8.3 \cdot 10^{14}$ cm^{-3}.

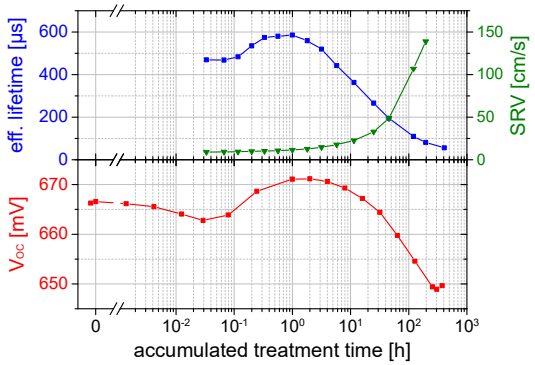

Figure 5: Comparison of the temporal evolution of open-circuit voltage (V_{oc}) of the PERC-type solar cell (bottom) as well as effective lifetime and surface recombination velocity (SRV) of the lifetime sample (top) during the accelerated aging test.

As mentioned in the sample description, boron-doped Cz-Si lifetime samples with both sided SiO_x/SiN_x:H passivation were prepared and fired. These samples were exposed to the similar accelerated aging test as the PERC-type solar cell. Figure 5 (top) shows the evolution of effective lifetime and effective surface recombination velocity (SRV). Even though the missing time resolution in the beginning conceals the ongoing BO-LID in the beginning, the increase in effective lifetime up to ~1 h is related to the regeneration from BO-LID. In the long-term, effective lifetime decreases significantly. In parallel, SRV is found to increase significantly thus the decrease in effective lifetime is caused by a deterioration of surface passivation quality. It is worth noting, that SRV did not show an increase due to BO-LID in the beginning, clearly demonstrating that the degradation in the long-term is caused by surface related degradation while degradation and subsequent regeneration in short-term are related to the bulk.

A comparison with the solar cell results (Fig. 5 bottom) shows the striking similarities of surface related degradation of the SiO_x/SiN_x:H passivation quality in the lifetime samples and the PERC-type solar cell suggesting that both suffer from basically the same phenomenon.

ACKNOWLEDGEMENTS

Part of this work was supported by the German Federal Ministry for Economic Affairs and Energy under Grants 0325877C, 0325763B and 0324001. The authors would like to thank A. Schwarz, L. Mahlstaedt, J. Lindroos, and M. Hagner for technical support as well as F. Huster for constructive discussions on loss mechanisms in solar cells. The content is the responsibility of the authors.

REFERENCES

[1] D. Sperber, A. Graf, D. Skorka, A. Herguth, G. Hahn
Degradation of surface passivation on crystalline silicon and its impact on light-induced degradation experiments
IEEE Journal of Photovoltaics **7** (2017) 1627
https://doi.org/10.1109/JPHOTOV.2017.2755072

[2] D. Sperber, A. Herguth, G. Hahn
On improved passivation stability on highly-doped crystalline silicon and the long-term stability of regenerated Cz-Si
Solar Energy Materials & Solar Cells **185** (2018), 277
https://doi.org/10.1016/j.solmat.2018.05.031

[3] D. Sperber, A. Schwarz, A. Herguth, G. Hahn
Enhanced stability of passivation quality on diffused silicon surfaces under light-induced degradation conditions
Solar Energy Materials & Solar Cells **188** (2018) 112
https://doi.org/10.1016/j.solmat.2018.08.019

[4] A. Herguth
On the meaning(fullness) of the intensity unit 'suns' in light induced degradation experiments
Energy Procedia. **124** (2017) 53
https://doi.org/10.1016/j.egypro.2017.09.339

[5] K. Bothe, R. Sinton, J. Schmidt
Fundamental boron-oxygen-related carrier lifetime limit in mono- and multicrystalline silicon
Progress in Photovoltaics: Res. Appl. **13** (2005) 287
https://doi.org/10.1002/pip.586

[6] T. Niewelt, J. Schön, W. Warta, S. Glunz, M. Schubert
Degradation of crystalline silicon due to boron-oxygen defects
IEEE Journal of Photovoltaics **7** (2017) 383
https://doi.org/10.1109/JPHOTOV.2016.2614119

[7] A. Herguth, G. Schubert, M. Kaes, G. Hahn
A new approach to prevent the negative impact of the metastable defect in boron doped Cz silicon solar cells
Proceedings of the 3rd World Conference on Photovoltaic Energy Conversion (2006) 940
https://doi.org/10.1109/WCPEC.2006.279611

[8] A. Herguth, C. Derricks, D. Sperber
A detailed study on light-induced degradation of Cz-Si PERC-type solar cells: Evidence of rear surface-related degradation
IEEE Journal of Photovoltaics **8** (2018) 1190
https://doi.org/10.1109/JPHOTOV.2018.2850521